Final Report

Title: Optimization of the Flapping Wing Systems for a Micro Air Vehicle

AFOSR/AOARD Reference Number: AOARD-09-4103

AFOSR/AOARD Program Manager: John Seo

Period of Performance: June 2009 - May 2010

Submission Date: September 2010

PI: Gyung-Jin Park, Hanyang University

1271 Sa 3-dong, Sangnok-gu, Ansan City, Gyeonggi-do 426-791, Korea

Report Documentation Page

Form Approved
OMB No. 0704-0188

1. REPORT DATE	2. REPORT TYPE	3. DATES COVERED
24 SEP 2010		

4. TITLE AND SUBTITLE	5a. CONTRACT NUMBER
Optimization of the Flapping Wing Systems for MAV	5b. GRANT NUMBER
	5c. PROGRAM ELEMENT NUMBER
6. AUTHOR(S)	5d. PROJECT NUMBER
Gyung-Jin Park	5e. TASK NUMBER
	5f. WORK UNIT NUMBER
7. PERFORMING ORGANIZATION NAME(S) AND ADDRESS(ES)	8. PERFORMING ORGANIZATION REPORT NUMBER
Hanyang University,1271 Sa 1-Dong, Ansan,Gyunggi-Do 426-791,Korea (South),NA,NA	**N/A**
9. SPONSORING/MONITORING AGENCY NAME(S) AND ADDRESS(ES)	10. SPONSOR/MONITOR'S ACRONYM(S)
	11. SPONSOR/MONITOR'S REPORT NUMBER(S)

12. DISTRIBUTION/AVAILABILITY STATEMENT

Approved for public release; distribution unlimited.

13. SUPPLEMENTARY NOTES

14. ABSTRACT

: The flapping wing of a micro air vehicle is optimized to enhance performance while some rigidity is kept with minimum mass. A work flow for the design of the flapping wing is defined. The performances to be enhanced are thrust coefficient and propulsive efficiency. The flapping kinematics of the flapping wing is determined by solving a path optimization problem which maximizes the performances. The optimization process is carried out based on a well defined surrogate model. The surrogate model is made from the results of two-dimensional fluid dynamic analysis. The Kriging method is employed to establish the surrogate model and a genetic algorithm is utilized for the multi-objective function problem. Dynamic topology optimization is performed to find the distribution of reinforcement. Certain rigidity can be kept by the results of topology optimization. A dynamic topology optimization method is developed by modification of the equivalent static loads method for non linear static response structural optimization. Three-dimensional computational fluid dynamic analysis is performed based on the optimum values of the path optimization to evaluate the external loads for the topology optimization process. It is found that the topology results are quite similar to the practical product. The process of the defined work flow is materialized by interfacing various software systems.

15. SUBJECT TERMS

16. SECURITY CLASSIFICATION OF:			17. LIMITATION OF ABSTRACT	18. NUMBER OF PAGES	19a. NAME OF RESPONSIBLE PERSON
a. REPORT	b. ABSTRACT	c. THIS PAGE			
unclassified	**unclassified**	**unclassified**		**29**	

(1) Objectives:

Recently, the research on the flapping micro air vehicle which imitates living creatures is being actively carried out. The objective of this research is the definition of the work flow for the design of the flapping wing. Generally, the best performance and the minimum mass should be pursued in the design of the flapping wing micro air vehicle. The flapping wing structure should have some rigidity which is kept with minimum mass. Therefore, path optimization is performed for maximizing the performance and dynamic topology optimization is performed for determining the distribution of the reinforcement. Reinforcement within the wing is determined to have certain rigidity with minimum mass. Dynamic topology optimization is performed based on the optimum values of path optimization.

(2) Status of effort:

This research starts from a well defined flapping wing which is proposed by Jones and Platzer in 2006. Path optimization is performed for a flapping wing. The objective function to be maximized is a multi-objective function which is composed of the thrust coefficient and the propulsive efficiency. In order to evaluate the objective function, computational fluid dynamics (CFD) analysis is used. A gradient based optimization is extremely expensive because of CFD analysis. Therefore, a surrogate model is utilized and the Kriging method is employed to establish the surrogate model. The design points (samples) are defined by an orthogonal array. A genetic algorithm is selected to solve the multi-objective function problem. For structural design, 3D unsteady CFD analysis is performed with the optimum values from the path optimization. The 3D unsteady CFD analysis results supply the pressure distribution in the time domain and this dynamic pressure distribution is used as the external loads for dynamic analysis of the flapping wing structure. Dynamic topology optimization is performed to find the distribution of reinforcement. A dynamic topology optimization method is developed by modification of the Equivalent Static Loads method for non linear static response Structural Optimization (ESLSO).

(3) Abstract:

The flapping wing of a micro air vehicle is optimized to enhance performance while some rigidity is kept with minimum mass. A work flow for the design of the flapping wing is defined. The performances to be enhanced are thrust coefficient and propulsive efficiency. The flapping kinematics of the flapping wing is determined by solving a path optimization problem which maximizes the performances. The optimization

process is carried out based on a well defined surrogate model. The surrogate model is made from the results of two-dimensional fluid dynamic analysis. The Kriging method is employed to establish the surrogate model and a genetic algorithm is utilized for the multi-objective function problem. Dynamic topology optimization is performed to find the distribution of reinforcement. Certain rigidity can be kept by the results of topology optimization. A dynamic topology optimization method is developed by modification of the equivalent static loads method for non linear static response structural optimization. Three-dimensional computational fluid dynamic analysis is performed based on the optimum values of the path optimization to evaluate the external loads for the topology optimization process. It is found that the topology results are quite similar to the practical product. The process of the defined work flow is materialized by interfacing various software systems.

(4) Personnel Supported:

Title	Name	Extra information
Professor	Gyung-Jin Park	Principal Investigation
Post Doctoral Fellow	Liangyu Zhao	CFD analysis, Path optimization
Ph.D. student	Jung-Sun Choi	Dynamic topology optimization

(5) Publications:

Choi, J. S., Zhao, L., Park, G. J., Agrawal, S. K., and Kolonay, R. M., "Enhancement of a Flapping Wing Using Path and Dynamic Topology Optimization," submitted to AIAA Journal (peer-reviewed publication)

(6) Interactions:

Conference

- Choi, J. S., Zhao, L., Park, G. J., Agrawal, S. K., and Kolonay, R. M., "Preliminary Research on Topology Optimization of the Flapping Wing," 6th China-Japan-Korea Joint Symposium on Optimization of Structural and Mechanical Systems, June 22-25, Kyoto, Japan, 2010.
- Zhao, L., Choi, J. S., Park, G. J., Agrawal, S. K., and Kolonay, R. M., "Multi-objective Path Optimization of Flapping Airfoils Based on a Surrogate Model," 6th China-Japan-Korea Joint Symposium on Optimization of Structural and Mechanical Systems, June 22-25, Kyoto, Japan, 2010.
- Choi, J. S., Zhao, L., Park, G. J., Agrawal, S. K., and Kolonay, R. M., "Topology Optimization of a Flapping Wing using Equivalent Static Loads," International Conference on Intelligent Unmanned Systems, Nov 3-5, Bali, Indonesia, 2010.

(7) Archival Documentation:

Path and Dynamic Topology Optimization for Design of the Reinforcement on Flapping Wing

Abstract

The flapping wing of a micro air vehicle is optimized to enhance performance while some rigidity is kept with minimum mass. A work flow for the design of the flapping wing is defined. The performances to be enhanced are thrust coefficient and propulsive efficiency. The flapping kinematics of the flapping wing is determined by solving a path optimization problem which maximizes the performances. The optimization process is carried out based on a well defined surrogate model. The surrogate model is made from the results of two-dimensional fluid dynamic analysis. The Kriging method is employed to establish the surrogate model and a genetic algorithm is utilized for the multi-objective function problem. Dynamic topology optimization is performed to find the distribution of reinforcement. Certain rigidity can be kept by the results of topology optimization. A dynamic topology optimization method is developed by modification of the equivalent static loads method for non linear static response structural optimization. Three-dimensional computational fluid dynamic analysis is performed based on the optimum values of the path optimization to evaluate the external loads for the topology optimization process. It is found that the topology results are quite similar to the practical product. The process of the defined work flow is materialized by interfacing various software systems.

Nomenclature

AR	=	aspect ratio
a	=	dimensionless length from the leading edge to the pivot point

$\mathbf{b}$	=	design variable vector
$\mathbf{C}(\mathbf{b})$	=	viscous damping matrix
CFD	=	computational fluid dynamics
C_D	=	drag coefficient
C_L	=	lift coefficient
C_T	=	thrust coefficient
C_M	=	pitch moment coefficient
$\bar{C}_D$	=	time average drag coefficient
$\bar{C}_L$	=	time average lift coefficient
$\bar{C}_T$	=	time average thrust coefficient
c	=	chord, m
E	=	Young's modulus
F_x	=	x component of the resulting aerodynamics force acting on the airfoil, N
F_y	=	y component of the resulting aerodynamics force acting on the airfoil, N
f	=	frequency, Hertz
$\mathbf{f}_{eq}(s)$	=	equivalent static loads vector
h	=	reduced plunging amplitude with respect to the chord
k	=	reduced frequency
$\mathbf{K}(\mathbf{b})$	=	stiffness matrix
$\mathbf{M}(\mathbf{b})$	=	mass matrix
Ma	=	mach number
Re	=	Reynolds number
S	=	reference area
St	=	Strouhal number
T	=	period, second
u	=	far field flow velocity, m/s
$\mathbf{v}_e$	=	volume of each element

V	=	total volume of the structure
$\mathbf{z}(t)$	=	dynamic displacement vector
$\mathbf{z}(s)$	=	static displacement vector
ϕ	=	phase angle of pitching motion leading plunging motion
ρ	=	density of fluid around the airfoil, kg/m^3
ρ_m	=	density of the material, kg/m^3
θ	=	angle between the chord and the far field flow speed direction
η	=	propulsive efficiency
ω	=	angular frequency, rad/s
ε_1	=	specified value of density
ε_2	=	percent of the total design variable
ε_3	=	density value of design update

I. Introduction

The flapping wing MAV (FWMAV), inspired by birds, bats, insects, fishes and whales, has been getting more and more attention from military and civilian application domains since the micro air vehicle (MAV) was generally defined by the Defense Advanced Research Projects Agency (DARPA) in 1997 [1]. Some unique advantages of FWMAVs, such as high maneuverability and hovering capability, make the research in this area quite active. Early studies, such as the Garrick theory [2], focused on simplified models. As research evolved, practical and sophisticated models are employed. The continuous development of computational methods makes it possible to simulate a real insect flying in the air [3] and some FWMAVs were fabricated during the past years. For example, Jones and Platzer proposed an unconventional biplane flapping wing MAV in 2006 [4]. In this model, the thrust is generated by the biplane pair of the two trailing flapping wings and the lift is generated by the front stationary wing as shown in Fig. 1. The present work is closely related to this design.

From the perspective of engineering, the best performance and the minimum mass should be pursued in the design of the FWMAV. The flapping path should be determined to maximize the performance. Recent experimental and computational achievements showed that the flapping performance, such as the thrust coefficient and the propulsive

efficiency, depends on the flapping kinematics significantly. Anderson showed that oscillating foil could have a very high propulsive efficiency, as high as 87%, under specific combinations of the flapping kinematics by water tunnel experiments [5]. Pesavento and Wang found that optimized flapping wing motions could save up to 27% of the aerodynamic power required by the optimal steady flight [6]. In 2005, Tuncer and Kaya employed the steepest ascent search algorithm to maximize a linear combination of the maximum thrust and the propulsive efficiency for flapping airfoils [7]. In 2007, Kaya and Tuncer performed optimization with a NURBS (Non-Uniform Rational B-Splines, NURBS) flapping path instead of a sinusoidal flapping path in their previous paper, and a gradient based search algorithm was employed to find the optimum [8]. In 2009, Kaya, Tuncer, Jones and Platzer, extended their optimization scheme to a biplane configuration [9]. Meanwhile, Soueid, Guglielmini, Airiau and Bottaro optimized the motion of a flapping airfoil using sensitivity functions. In Soueid's work, the objective was a combination of several concerned parameters, such as the time average thrust coefficient, the average power input and the average angle of attack [10].

In this research, path optimization is performed based on the paradigm of the previous researches [7]; however, different optimization methods are utilized to reduce the effort for path optimization. A surrogate model is utilized in the optimization process and the Kriging method is employed to make the surrogate model [11]. The surrogate model is established by using 2-dimensional computational fluid dynamics (2D CFD) analysis because 3D CFD analysis in the optimization process is uncontrollably expensive. The surrogate model has the advantage over a gradient based optimization in that sensitivity analysis is not necessary. It is well known that sensitivity information from CFD analysis is extremely expensive. In other words, the surrogate model is used to reduce the computational cost. Since the objective function is a multi-objective function defined by the thrust coefficient and the propulsive efficiency, a genetic algorithm is utilized [12]. Moreover, the genetic algorithm can find a global solution while a gradient based optimization can find a local optimum.

Topology optimization is carried out to keep certain rigidity of the flapping wing with minimum mass. It is noted that there are not many studies on the structural design of the flapping wing. Some researchers have conducted topology optimization of the fixed wing of MAV [13]. In this research a topology optimization method is newly developed for the flapping wing. Topology optimization determines the distribution of the reinforcement on the flapping wing. The distribution of the reinforcement can be regarded as the vein distribution of the wing which mimics the wing of an insect. We need pressure distribution on the flapping wing. Since 2D CFD analysis does not

provide pressure distribution on the entire body, 3D CFD analysis is performed based on the optimum values of path optimization. The pressure from the 3D CFD analysis is imposed on the flapping wing as the external loads in the topology optimization process. It is noted that the pressures are imposed in the time domain; therefore, we need dynamic topology optimization. Generally, topology optimization is performed in a static sense. A dynamic topology optimization method is developed based on modification of a method called the Equivalent Static Loads method for non linear static response Structural Optimization (ESLSO) [14-16].

The problem is solved by interfacing various software systems. The commercial computational fluid dynamics (CFD) system, FLUENT [17], is utilized for unsteady aerodynamics analysis. NASTRAN [18] is used for dynamic analysis and GENESIS [19] is used for topology optimization. The optimization process uses the genetic algorithm in MATLAB [20]. An in-house C++ program [21] is coded to link the systems. The research results are summarized and the future direction for the design of the flapping wing is proposed.

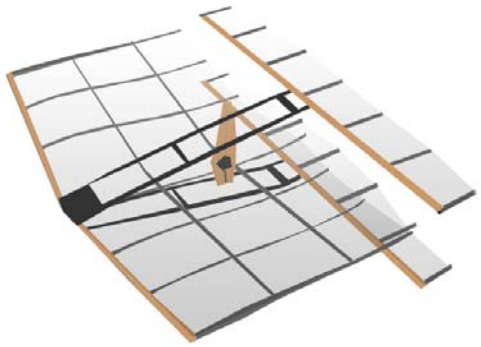

Fig. 1 Flapping-wing MAV model.

II. Flow of the Present Research

This work starts from a well defined flapping wing illustrated in Fig. 1. The biplane pair of the trailing wings is flapping and generates the thrust force. Path optimization is performed for a wing of the two flapping wings. The overall work flow is presented in Fig. 2. An optimization problem to determine the path is formulated. The motion of the flapping wing consists of the plunging motion and the pitching motion. The parameters for the path are the plunging amplitude, pitching amplitude and the phase angle between the two motions, and these parameters are used as design variables in path optimization. The objective function to be maximized is a multi-objective function

which is composed of the thrust coefficient and the propulsive efficiency. CFD analysis is required to evaluate the objective function. A gradient based optimization process needs sensitivity information with respect to design variables and it is well known that sensitivity analysis with CFD analysis is extremely expensive [10]. Therefore, a surrogate model is utilized in this research and the Kriging method is employed to establish the surrogate model [11]. Because 3D analysis is highly costly, 2D unsteady CFD analysis is conducted for the establishment of the surrogate model.

Responses such as the thrust coefficient and the propulsive efficiency are evaluated at various design points. The design points (samples) are defined by an orthogonal array. The surrogate model from the Kriging method is used in the optimization problem. A genetic algorithm is selected to solve the multi-objective function problem [12]. The genetic algorithm may not be practical if we directly use CFD analysis because the algorithm requires many function calculations. Since the surrogate model is utilized, the function calculation in the optimization process is almost negligible.

For structural design, the pressures on the flapping wing are required because they should be used as external loads on the structure. Only 3D CFD analysis can provide the pressure distribution around the flapping wing. Therefore, a computational model in three dimensions is made and 3D unsteady CFD analysis is performed with the optimum values from the path optimization. The flapping motion is dynamic (transient) and we need the pressure distribution in the time domain. The 3D unsteady CFD analysis results supplies the pressure distribution in the time domain and this dynamic pressure distribution is used as the external loads for dynamic analysis of the flapping wing structure.

The flapping wing structure should have some flexibility as well as certain rigidity [22-23], and a small amount of rigidity guarantees flexibility. Topology optimization is performed to satisfy this condition with minimum mass. The reinforcement in the flapping wing can be determined in the topology optimization process. The reinforcement can be regarded as the vein distribution of the wing if the flapping wing mimics that of an insect. Topology optimization is generally carried out with static loads [24]. However, the flapping wing operates in the dynamic (transient) environment. Therefore, the current topology optimization methods can be hardly used for the design of the flapping wing. A topology optimization method is developed to handle the dynamic pressure distribution in the time domain. The new method is a modified version of the Equivalent Static Loads method for non linear static

response Structural Optimization (ESLSO) [25]. ESLSO has been extensively used for size and shape optimizations and it is modified for topology optimization in this research.

The logic for the current work may not be perfect because of the cost and the limitation of the technical problems. For example, if optimization with 3D aeroelasticity analysis is used, the path and the structure can be optimized simultaneously. However, this approach does not seem to be realistic at this moment. Moreover, the pair of the flapping should be considered together. The future direction of this research is proposed in a later section.

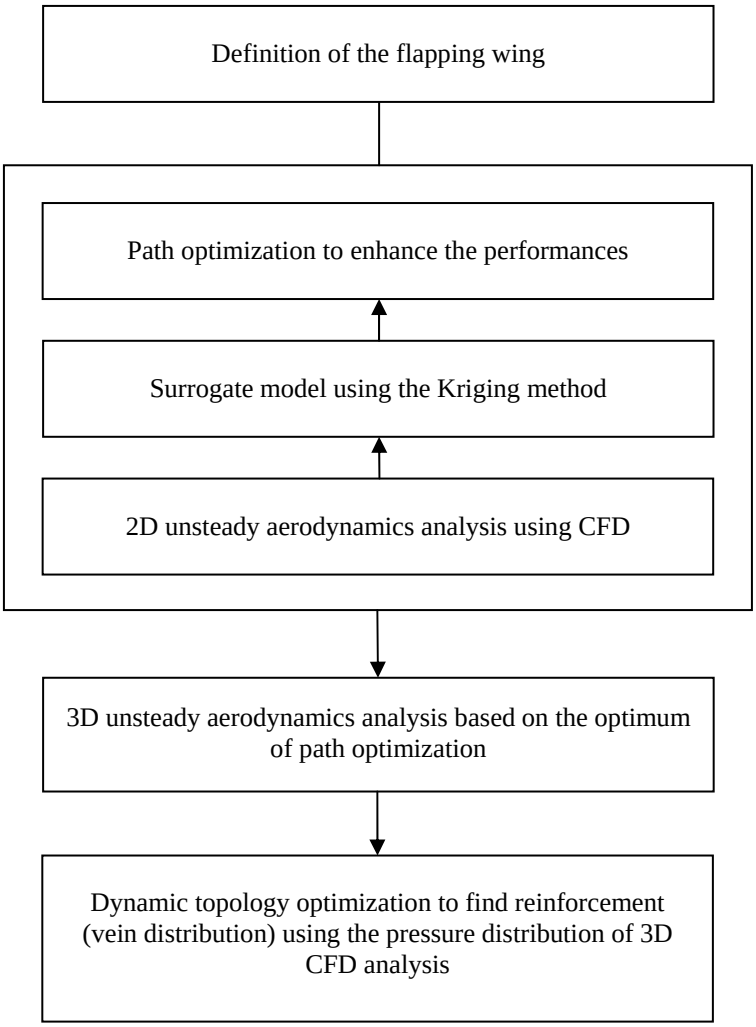

Fig. 2 Flow of the research.

III. Path Optimization

This section starts with the description of the flapping motion. The involved governing equations and a well validated mesh for simulating the unsteady flow field around an airfoil are also described. After the path optimization problem is defined, the surrogate model for the Kriging method is carefully constructed. Then, the optimum flapping kinematic parameters are obtained by a genetic algorithm. At the end of this section, 3D CFD analysis is performed under these optimum parameters for a wing with a given aspect ratio. Meanwhile, the derivations between flapping performances of the 2D airfoil and ones of the 3D wing are demonstrated.

A. Flapping Wing System

The flapping motion, including the plunging and pitching motions, can be described as follows:

$$y(t) = hc\cos(\omega t) \tag{1}$$

$$\theta(t) = \theta_0 \cos(\omega t + \phi) \tag{2}$$

where $y(t)$ stands for the plunging motion, $\theta(t)$ the pitching motion, c is the chord length, h is the dimensionless plunging amplitude, ω is the angular frequency in rad/s, θ_0 is the pitching amplitude and ϕ is the phase shift angle of the pitching motion leading the plunging motion. The reduced frequency k, is defined as

$$k = 2\pi fc / u = \omega c / u \tag{3}$$

where f is the flapping frequency in Hertz and u is the flow velocity of the far field. This flapping model is illustrated using a 2D airfoil in Fig. 3, where O is the pivot point and a is the dimensionless length from the leading edge to the pivot point with respect to the chord.

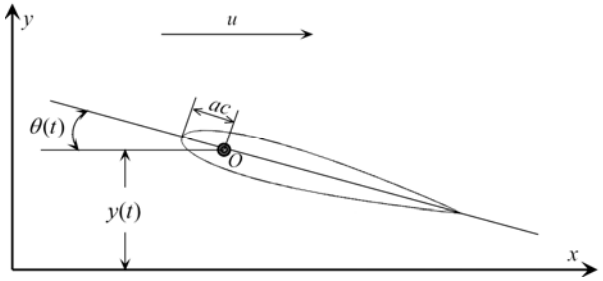

Fig. 3 Illustration of the flapping model.

The Reynolds number (Re) and the Strouhal number (St) are

$$Re = \rho uc / \mu \tag{4}$$

$$St = fA / u \tag{5}$$

where ρ is the fluid density, μ is the fluid dynamic viscosity and A is the wake width and can be estimated using the peak-to-peak excursion of the trailing edge, or more simply by twice the plunging amplitude.

In classical aerodynamics, the lift coefficient C_L, the drag coefficient C_D, and the pitch moment coefficient C_M can be defined as

$$C_D = \frac{F_x}{0.5\rho u^2 S} \tag{6}$$

$$C_L = \frac{F_y}{0.5\rho u^2 S} \tag{7}$$

$$C_M = \frac{M_z}{0.5\rho u^2 SL} \tag{8}$$

where F_x and F_y are the components of the resulting aerodynamics force along horizontal (parallel with u direction) and vertical (normal to u direction) directions, respectively, S is the reference area and equals to c in value for a 2D problem, M_z is the pitch moment with respect to the pivot point and L is the reference length and equals to c here. The time-average thrust coefficient $\bar{C}_T$ and the power input coefficient $\bar{C}_P$ in one flapping cycle can be calculated by Eqs. (9)-(10). Correspondingly, the propulsive efficiency is defined in Eq. (11).

$$\bar{C}_T = -\bar{C}_D = -\frac{1}{T}\int_t^{t+T} C_D(t)dt\,, \tag{9}$$

$$\bar{C}_P = \frac{1}{T}\left(\int_t^{t+T} C_L(t)\dot{y}(t)dt + \int_t^{t+T} C_M(t)\dot{\theta}(t)cdt\right), \tag{10}$$

$$\eta = \bar{C}_T u / \bar{C}_P\,, \tag{11}$$

where T is the period in *seconds* with $T = 1/f$ and $\dot{y}(t)$ and $\dot{\theta}(t)$ are the first order time derivation of $y(t)$ and $\theta(t)$, respectively. For simplicity, we also use C_D to stand for $\bar{C}_D$, C_T for $\bar{C}_T$ in the next sections.

B. Two Dimensional CFD Analysis

The commercial CFD solver FLUENT [17] is employed to simulate the unsteady flow fields around the moving wings with predefined motions. The time-dependent Navier-Stokes equations are solved using the finite volume method, assuming incompressible laminar flow. The mass and momentum equations are solved in a fixed inertial reference frame incorporating a dynamic mesh. The continuity and the momentum equations are given as

$$\nabla \cdot \boldsymbol{V} = 0\,, \tag{12}$$

$$\rho\left(\frac{\partial \boldsymbol{V}}{\partial t} + \boldsymbol{V}\cdot\nabla\boldsymbol{V}\right) = -\nabla p + \mu\nabla^2\boldsymbol{V}\,, \tag{13}$$

where $\boldsymbol{V}$ and p are velocity and pressure, respectively.

The hybrid mesh which is shown schematically in Fig. 4 is employed to compute the flow field. The computational domain is divided into two distinct zones: moving zone and re-meshing zone. The moving zone consists of the C-type structured quadrilateral mesh, and the re-meshing zone consists of the unstructured triangular mesh. The airfoil is located in the center of the computational domain, and the no-slip wall boundary condition is applied. The spatial scale of each zone and corresponding boundary condition are also shown in Fig. 4. The whole moving zone mesh, including the interfaces between these two zones, moves with the airfoil together according to the predefined airfoil motion. This means re-meshing only occurs at a distance of 20 to 45 reference lengths away from the airfoil body, which insures that the flow simulation around the airfoil is somewhat affected by the moving mesh. The C-type mesh structure in the very close neighborhood of the airfoil is shown in Fig. 5, and the grid size is 201×101 nodes (201 along every single airfoil surface, 101 in the vertical direction) with the thickness of the first layer grid around the airfoil equal to 0.0002*c*. The hybrid mesh is generated in GAMBIT v2.3.16 [26].

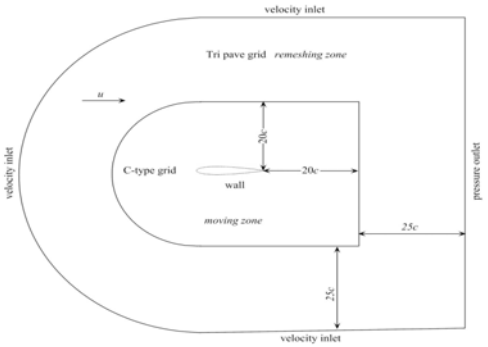

Fig. 4 Hybrid mesh topology with boundary conditions.

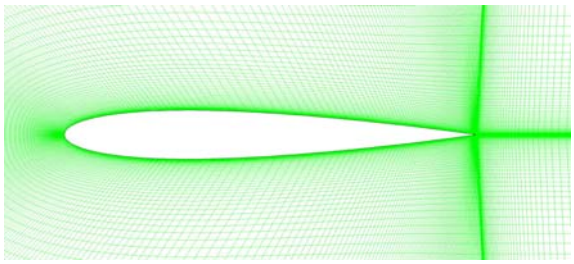

Fig. 5 C-type grid very close to the airfoil.

To validate the accuracy of the present approach, simulations are performed in 7 periods with 500 and 1000 time steps in one plunging period under the conditions of k=2.0, h=0.4, u=34.7 m/s (Ma=0.1), c=0.064 m, and Re=1.0×10^4 respectively. The coupling between the pressure and the velocity is achieved by means of the SIMPLEC algorithm. Meanwhile, the discretizations of pressure and momentum terms are the Second Order scheme and the Second Order Upwind scheme. The time discretization is the First Order Implicit scheme, which is a more straightforward method in FLUENT for the dynamic mesh module [27]. The time variation of the plunging position and the time histories of C_D in one period are shown in Fig. 6, with the comparisons with results obtained by Tuncer [28] and Miao [22]. These four results have a good agreement, though different mesh schemes are employed in these studies. Figure 6 also shows that 500 time steps in one cycle are good enough to get the concerned details. Based on the validation, 201×101 size grid with the first layer thickness of 0.0002c, and 500 time steps are employed for all of the simulations in the next sections.

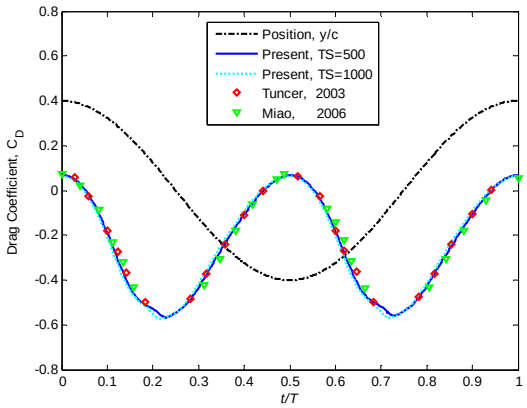

Fig. 6 Validation for the plunging motion.

C. Optimization Formulation

The path optimization problem for a NACA0012 airfoil [7] is formulated under the flight conditions of $k = 1$, $u = 3.0$ m/s, $c = 0.05$ m, and $Re = 1e4$ as follows:

$$\text{Find} \qquad h,\ \theta_0, \phi$$

$$\text{to minimize} \qquad f(h,\ \theta_0, \phi) = (1-\beta)\frac{C_T - C_{T,\max}}{C_{T,\min} - C_{T,\max}} + \beta\frac{\eta - \eta_{\max}}{\eta_{\min} - \eta_{\max}} \tag{14}$$

$$\text{subject to} \qquad 0.8 \le h \le 2.5,\ 10.0 \le \theta_0 \le 30.0,\ 80.0 \le \phi \le 135.0$$

where β is the weight factor, $C_{T,\min}$ and $C_{T,\max}$ are the minimum and the maximum time average thrust coefficients in the design array for constructing the Kriging model, and $\eta_{\min}$ and $\eta_{\max}$ are the minimum and the maximum propulsive efficiency in the design array for constructing the Kriging model. This objective function is equivalent to maximizing the time average thrust coefficient and the propulsive efficiency simultaneously under the given weight factors.

D. Surrogate Model with the Kriging Method

In this research, the Kriging model is employed as the approximation method, and the orthogonal array as the design of experiments technique. The Kriging method initiated from the geostatistical field can be considered as a member of the family of linear least square estimation algorithms [11]. The Kriging model combines a global polynomial model plus a localized departure. This is why the Kriging model is expected to find a well global approximation at an unobserved location for a nonlinear problem [11, 12]. Based on the design space described, *h* is divided into 7 levels, θ_0 5 levels, and ϕ 6 levels as shown in Table 1. The design array in this paper consists of the union of the 49 samples obtained using a classical orthogonal array and the 8 vertices, which means 55 samples total. The high fidelity results are obtained using FLUENT under the given flight conditions.

In order to make the surrogate model be more flexible, two Kriging models are constructed to fit the time average thrust coefficient and propulsive efficiency, respectively. Five design points not belonging to the samples are selected to evaluate these two surrogate models as shown in Table 2. The largest relative error between the high fidelity model and the surrogate model is 5.3%, and these two Kriging models are supposed to be good enough to predict the time average thrust coefficient and the propulsive efficiency.

Table 1 Design space, factors and levels

No.	1	2	3	4	5	6	7
h	0.80	1.00	1.20	1.50	1.80	2.00	2.50
θ_0 (deg)	10.00	15.00	20.00	25.00	30.00		
ϕ (deg)	80.00	90.00	100.00	110.00	120.00	135.00	

Table 2 Validation of the Kriging models

No.	h	θ_0 (deg)	ϕ (deg)	C_D (sModel)	C_D (FLUENT)	Error	η (sModel)	η (FLUENT)	Error
1	1.60	23.50	103.40	-1.399019	-1.449604	3.50%	0.297454	0.296856	0.20%
2	1.36	29.60	97.80	-1.159442	-1.138866	1.80%	0.451900	0.476958	5.30%
3	1.73	23.80	100.70	-1.554946	-1.591267	2.30%	0.280245	0.277590	1.00%
4	1.52	26.90	87.20	-1.201629	-1.218762	1.40%	0.341126	0.355931	4.20%
5	1.55	28.60	94.90	-1.423153	-1.468366	3.10%	0.374416	0.390918	4.20%

E. Optimization Results

The weight factor β, is set to be 0.5, and the *ga* function embedded in MATLAB [20] is employed to solve the optimization problem. The optimization history is presented in Fig. 7. Correspondingly, the time average thrust coefficient and the propulsive efficiency are 1.10 and 0.4731, and the optimum design point is $h = 1.3265$, $\theta_0 = 30.0$, and $\phi = 97.6624$. It should be mentioned that this optimum is similar to Tuncer's optimum with $\beta = 0.5$ [7].

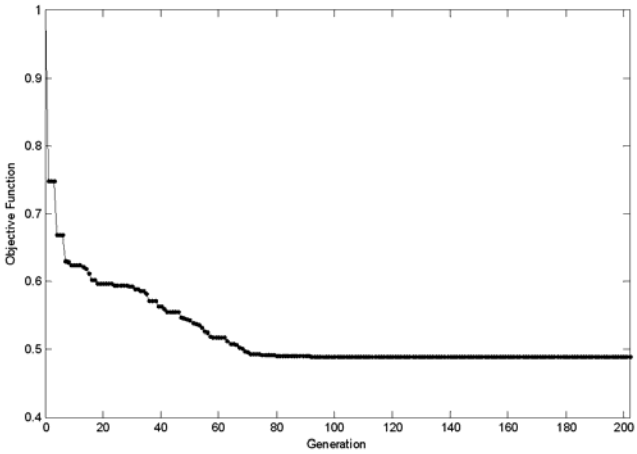

Fig. 7 Convergent history of the genetic algorithm.

F. Three Dimensional CFD Analysis

The grid near the 3D wing is shown in Fig. 8, and this 3D hybrid grid is validated using a 3D wing with pure plunging motion under the conditions of k=3.64, h=0.175, u=0.3 m/s, c=0.1 m, b(semi-span)=0.3 m, and Re=3.0×10^4. The results are compared with Heathcote's experimental results [23] and Tang's computational results [29] illustrated in Fig. 9. Both of the present results and Tang's results have a little derivation from the experimental results. However, the present results match well with the previous computational results.

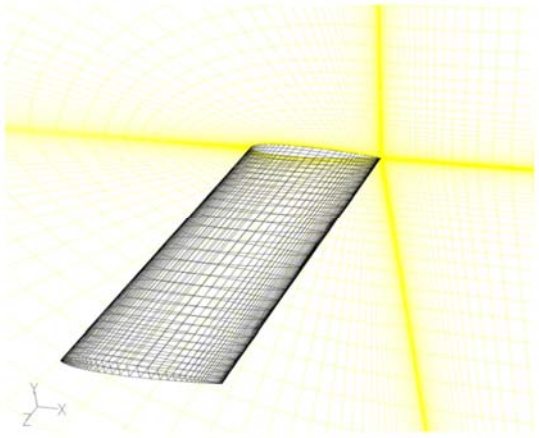

Fig. 8 A structured grid very close to the wing.

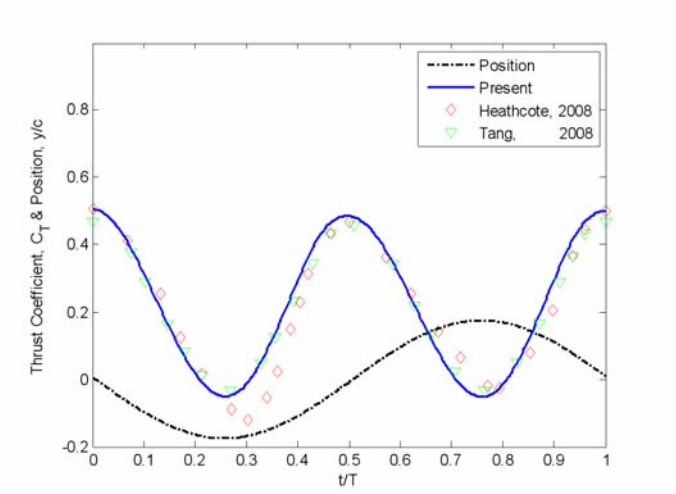

Fig. 9 Validation for a wing with pure plunging motion.

In the case of 2D computations, the wing tip vortexes and the spanwise flows are ignored compared to the 3D simulations. However, we still can expect that the 2D results are an acceptable approximation of the 3D results [30]. A wing with *AR*=6 and the optimum kinematic parameters are simulated. The time average thrust coefficient and the propulsive efficiency are shown in Table 3. It is observed that C_T and η obtained by the Kriging model and FLUENT at the optimum are very similar (the relative error is less than 5.5%). This validates the Kriging model again. The optimum of the 2D problem is assumed to be the optimum kinematic parameters for the 3D wing, though they have a little derivation in the time average thrust coefficient, up to 13.24%. Topology optimization in the next sections is based on this optimum.

Table 3 Comparison between 2D and 3D results

No.	h	θ_0	ϕ	C_T(Kriging)	C_T(FLUENT)	η(Kriging)	η(FLUENT)
2D	1.3265	30.0000	97.6624	1.1000	1.0705	0.4731	0.5001
3D	1.3265	30.0000	97.6624	--	0.9453	--	0.4992

IV. Topology Optimization

As mentioned earlier, the flapping motion is described by the pitching motion and plunging motion. The flapping motion is optimized by path optimization. The unsteady aerodynamics analysis is performed using the results of path optimization. The dynamic pressures of the surface are obtained. The pressures are applied to the finite element model of the wing for topology optimization. Topology optimization is used to find the optimal lay-out of a structure within a specified region. In general, the objective function to be minimized in topology optimization is the compliance with an equality constraint upon the volume fraction. Therefore, topology optimization is performed using the results of path optimization in order to reduce the weight and maximize stiffness to find the distribution of reinforcement.

A. Finite Element Model of the Flapping Wing

The surface pressures are obtained by using the optimum values of path optimization. First, the finite element model is generated based on the grid scheme of the unsteady aerodynamics analysis. However, the finite element model is not suitable for structure analysis because the aspect ratio of the elements is too high. Therefore, the grid is changed for structural analysis and Fig. 10 shows the finite element models. All the element pressures of Fig. 10 a) are obtained from unsteady aerodynamics analysis. The pressures are mapped to the finite element model for structural analysis using a 0-order interpolation as illustrated in Fig. 10.

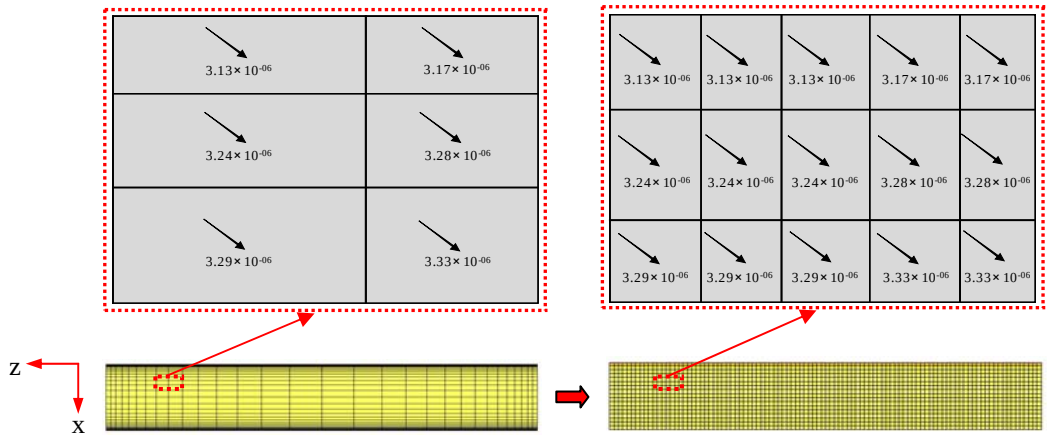

a) **b)**

Fig. 10 Application of the pressures of the finite element model: a) unsteady aerodynamic analysis model, b) structure analysis model.

Figure 11 presents the finite element model of the wing for topology optimization. In the flapping wing, the center point of the leading edge is attached to the frame as illustrated in Fig. 1. The boundary condition is imposed on the 13 nodes of the center. All the degrees of freedom in the six directions are fixed. The finite element model is composed of two shell element layers as illustrated in Fig. 12. In Fig. 12, the finite element model is divided into the design domain and the non-design domain.

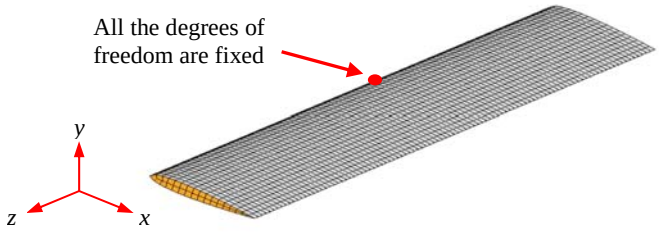

Fig. 11 The finite element model of the wing for topology optimization.

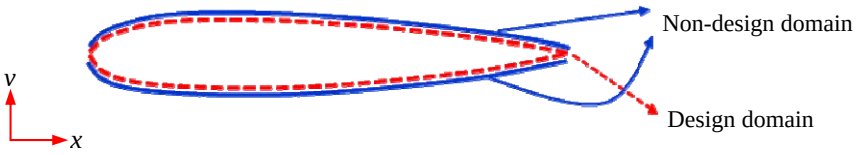

Fig. 12 The design and non-design domain for topology optimization.

The design domain is the inner layer of the shell elements. One layer is composed of 3,464 shell elements. Common nodes are used for the outer and inner shell elements. The Young's modulus of the design domain (carbon) is 170.3 GPa, the Poisson's ratio is 0.3 and material density is 2001.2 kg/m^3. The Young's modulus of the non-design domain (mylar) is 3.28 GPa, the Poisson's ratio is 0.4 and material density is 1400.6 kg/m^3. The thickness of the design domain is 1.0 mm and the thickness of the non-design domain is 0. 1 mm. The pressures are always applied on the non-design domain and the non-design domain is supported by the design domain. Therefore, the topology of the reinforcement (carbon) is changed during the iteration of topology optimization.

In order to perform dynamic topology optimization, the surface pressures are calculated at every time step of dynamic analysis. The pressures are applied to the finite element model.

B. General Formulation of Topology Optimization

Topology optimization determines the state of material distribution in the structural domain. The intermediate variable is used for the design variables in the density method and has a value from 0 to 1. These design variables determine the existence of the materials. An element does not exist when the value of the design variable is zero and exists when the value of the design variable is 1 [31]. The general purpose of topology optimization is to maximize stiffness. The objective function is the average compliance and the design variables are the intermediate density variables. The topology optimization formulation is as follows:

$$\begin{aligned} &\text{Find} && \mathbf{b} \\ &\text{to minimize} && \text{compliance} \\ &\text{subject to} && \textstyle\sum \mathbf{v}_e \mathbf{b} \le V \\ & && 0 < \mathbf{b}_{\min} \le \mathbf{b} \le 1 \end{aligned} \tag{15}$$

where the design variable vector $\mathbf{b}$ is the density of elements, $\mathbf{v}_e$ is the volume of each element, and V is the total volume of the structure. Mainly, strain energy is used for the objective function as compliance in linear static topology optimization because compliance is twice as large as strain energy.

The design variables in topology optimization do not directly correspond to the existence of the material. Therefore, the material property update method is utilized to use the results of the previous iteration in the next iteration. The update rule of the material property of each element is as follows [31]:

$$\mathbf{E} = \mathbf{b}^{(k)^p} \mathbf{E}_0 \tag{16}$$

$$\boldsymbol{\rho}_m = \mathbf{b}^{(k)^q} \boldsymbol{\rho}_0 \tag{17}$$

$\mathbf{E}$ is the Young's modulus vector for all the elements and it represents the stiffness of an isotropic elastic material. $\boldsymbol{\rho}_m$ is the vector for the density of the material. The value of $\mathbf{E}_0$ means the initial Young's modulus and the value of $\boldsymbol{\rho}_0$ means the initial density of the material. In general, the value of p is 2 or 3 and the value of q is 1 [24]. This update method for the material property is used each iteration in the commercial software system. Static topology optimization proceeds this way.

C. Formulation of Dynamic Topology Optimization

All the forces in the real world act dynamically on structures. The surface pressures of the wing are changed in accordance with the time during the flapping motion. Thus, design and analysis should be performed based on the dynamic loads. Dynamic topology optimization is performed to find the distribution of reinforcement on the flapping wing.

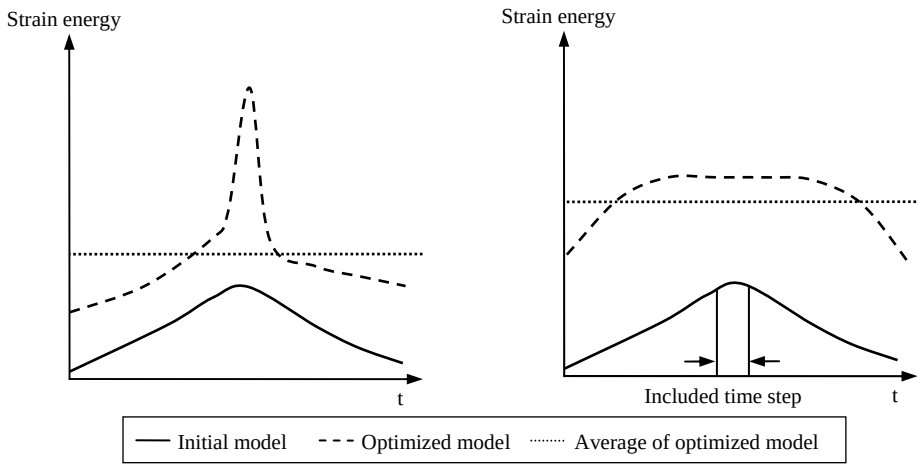

a) **b)**

Fig. 13 The graph of the strain energy: a) minimization of summations, b) minimization of the peaks.

In dynamic topology optimization, some researchers claimed that the summation of the strain energy is minimized during the entire time [25, 32]. Dynamic topology optimization is carried out for the stiffest structure with a specific mass in the time domain. Figure 13 shows examples of the strain energy between the initial model and the optimized model. The initial model has a 100 percent mass of the structure and the optimized model has a specific mass according to the constraint on the mass fraction. Thus, the strain energy of the optimized model is larger than that of the initial model under the same dynamic load.

Figure 13 a) shows the minimization of strain energy summation during the entire time and Fig. 13 b) shows the minimization of the peak values of the strain energy. In the optimized model, the strain energy of Fig. 13 a) increases rapidly at a particular time, while the average strain energy of Fig 13 a) is smaller than that of Fig 13 b). It means that the deformation of the structure can be very large at a particular time. In Fig. 13 b), the average of the strain energy is larger, while the peak is smaller. This means that the deformation of the case in Fig. 13 b) is uniform in the time domain. Since a large deformation for even a short time is dangerous to the flapping motion, the

peaks of the strain energy are minimized in dynamic topology optimization. The peaks of the strain energy are found by dynamic analysis. As the design proceeds, the peaks of the current iteration may not be the peaks in the next iteration. Thus, the strain energies for a few time steps near the peaks are minimized as illustrated in Fig. 13 b). During the included time steps, the summation of strain energy is minimized. The peaks of strain energy are decreased and the topology of the structure is obtained for a specific mass.

A dynamic optimization method has been developed for size and shape optimizations based on ESLSO. ESLSO includes dynamic characteristics without complex differential equations. The efficiency of ESLSO has been verified by various researches [16, 33-37]. As mentioned earlier, ESLSO is expanded for dynamic topology optimization of the flapping wing. Equivalent static loads (ESLs) are made to generate the same response field as that from dynamic pressures at each time step of unsteady aerodynamics analysis. At the time steps near the peaks of the strain energy, ESLs are calculated and ESLs are used as the external pressures in static topology optimization.

Dynamic topology optimization using ESLs is formulated as follows:

$$\begin{aligned} &\text{Find} && b_i; && i = 0, \ldots, 3200 \\ &\text{to minimize} && \text{peaks of strain energy} \\ &\text{subject to} && \text{mass} \le \text{mass}_{\text{initial}} \times 0.2 \\ & && 0 < b_{i\,\min} \le b_i \le 1.0 \end{aligned} \tag{18}$$

The design variable b_i is the design variable of the ith element in the design domain. The objective function is the summation of the strain energy at the time steps near the peaks of the strain energy. The constraint is that the mass of the structure should be less than 20 percent of the initial mass.

D. ESLSO for Topology Optimization

ESLSO is a method for dynamic optimization on structures. The loads that are made to generate the same displacement field as dynamic loads at each time steps are called ESLs. The ESLs consider all the behaviors of a structure through time. Then the ESLs are applied to static optimization because the loads remove the time dependent constraint conditions. Calculated ESLs at each time step are used as multiple loading conditions in

topology optimization. The process of calculating ESLs is explained. The governing equation of dynamic analysis is

$$\mathbf{M}(\mathbf{b})\ddot{\mathbf{z}}(t) + \mathbf{C}(\mathbf{b})\dot{\mathbf{z}}(t) + \mathbf{K}(\mathbf{b})\mathbf{z}(t) = \mathbf{f}(t); \qquad t = 0,\cdots,l \tag{19}$$

where $\mathbf{M}(\mathbf{b})$ is the mass matrix, $\mathbf{C}(\mathbf{b})$ is the damping matrix, $\mathbf{K}(\mathbf{b})$ is the stiffness matrix, $\mathbf{z}(t)$ is the dynamic displacement vector, t is the time and l is the number of time steps. ESL is calculated as

$$\mathbf{f}_{eq}(s) = \mathbf{K}(\mathbf{b})\mathbf{z}(s); \qquad s = 0,\cdots,l \tag{20}$$

where $\mathbf{f}_{eq}(s)$ is the ESLs vector, $\mathbf{K}(\mathbf{b})$ is the stiffness matrix and s is the loading case which is equivalent to t in Eq. (19). The number of ESLs is the same as that of the time steps.

ESLSO was originally developed for size/shape optimization. A preliminary study on topology optimization using ESLs was performed for a small scale standard problem [25]. As mentioned earlier, since the summation of the strain energy in the entire time domain was minimized, the optimum topology was not practical. In this research, the method is modified to minimize the peaks and applied to the design of a flapping wing. The process of topology optimization using ESLSO is as follows:

Step 1. Set cycle number $k = 0$, and the design variables $\mathbf{b}^{(k)} = \mathbf{b}^{(0)}$.

Step 2. Perform dynamic analysis with $\mathbf{b}^{(k)}$.

Step 3. Calculate ESLs in the time domain by using Eq. (20).

Step 4. Perform static topology optimization as follows:

$$\begin{aligned} &\text{Find} && \mathbf{b} \\ &\text{to minimize} && f(\mathbf{b},\mathbf{z}) \\ &\text{subject to} && \mathbf{K}(\mathbf{b})\mathbf{z}(s) = \mathbf{f}_{eq}(s); \qquad s = 1,\cdots,q \\ & && g_j(\mathbf{b},\mathbf{z}) \le 0; \qquad j = 1,\cdots,m \\ & && 0 < \mathbf{b}_{\min} \le \mathbf{b} \le 1 \end{aligned} \tag{21}$$

where the design variables are the density of each element and the objective function is the summation of strain energy at the time steps near the peaks of the strain energy.

Step 5. When $k = 0$, go to Step 6. Otherwise, check the convergence.

If the convergence criterion is satisfied, the optimization process terminates. If the convergence criterion is not satisfied, go to Step 6.

Step 6. Update the design, set $k = k + 1$, and go to Step 2.

The process is repeated until the convergence criterion is satisfied. The repetition process is called a cycle. The difference of dynamic and static responses is decreased as the repetition proceeds. The overall process is illustrated in Fig. 14.

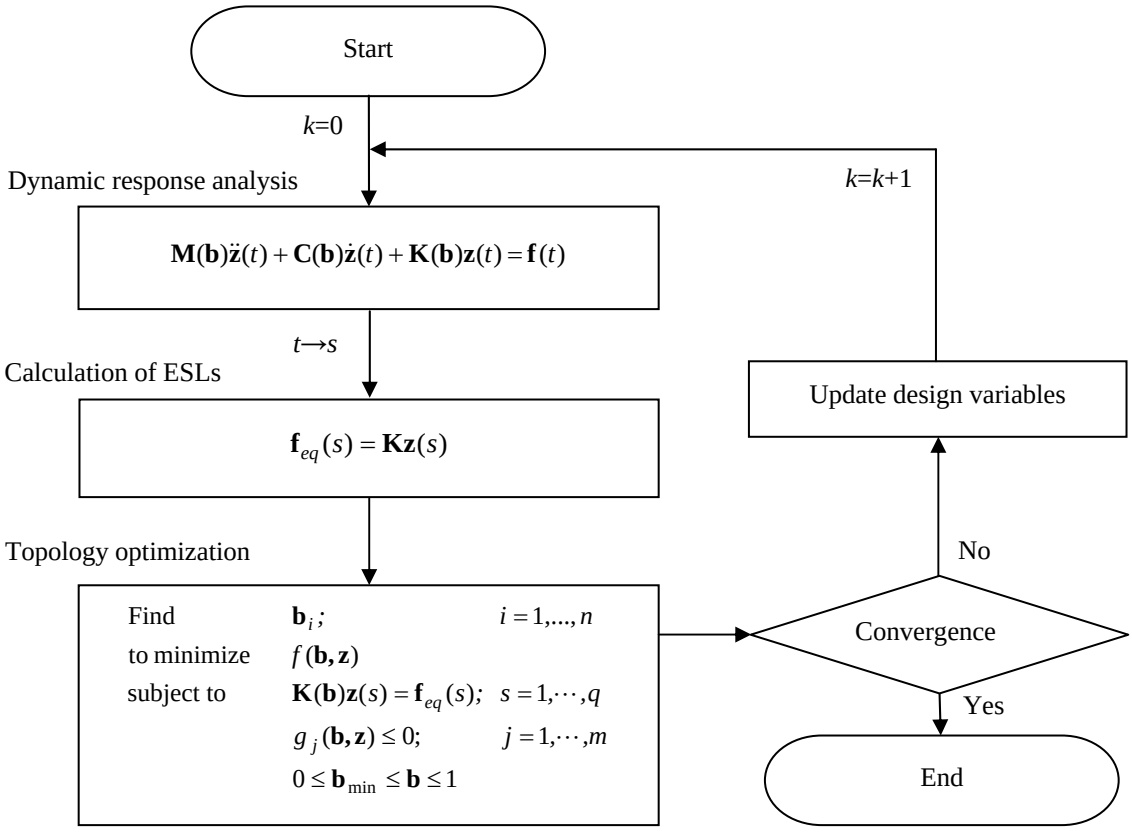

Fig. 14 The process of topology optimization using ESLSO.

1. Convergence Criterion

A convergence criterion can be defined by borrowing the existing one for size and shape optimizations. It is defined as

$$\sum_{i=1}^{n}\left|b_i^{(k)}-b_i^{(k-1)}\right|\le\varepsilon_1 \tag{22}$$

where ε_1 is a user-defined small number. Equation (22) is checked in Step 5. After static topology optimization, if the change of design variables from the previous cycle is small, the process terminates. However, it is difficult to satisfy this condition in topology optimization because some design variables have a repeated value of 0 and 1. Therefore, a new convergence criterion is defined as

$$countif\left(\left|b_i^{(k)}-b_i^{(k-1)}\right|\ge\varepsilon_1\right)\le n\times\varepsilon_2 \tag{23}$$

where ε_2 is another user-defined small number. In Eq. (23), the number of design variables which change more than ε_1 is counted first. If the counted number is less than certain value $n\times\varepsilon_2$, then the process terminates. The convergence criterion in Eq. (23) is utilized.

2. Method for Design Update

In general static topology optimization, the update method of the material property is in Eqs. (16)-(17). However, this update method is used within static topology optimization. The update method between the cycles is newly defined for dynamic topology optimization. The optimum design variables from static topology optimization have the values in the continuous apace from 0.0 to 1.0. After static topology optimization is finished, the elements less than a user defined small number ε_3 are removed and the design variables for the elements larger than ε_3 are remained. It is noted that ε_3 should be fairly small because the results with a large ε_3 deteriorate the connectivity of the elements. Even a small ε_3 removes elements quite a lot. The density of an element is changed so that a removed element has 0.0 and the remained element has 1.0. The new density is updated and dynamic analysis is performed with the new densities in the next cycle.

E. Results of Topology Optimization

As mentioned earlier, dynamic topology optimization is performed to find the reinforcement of the flapping wing. The dynamic pressure from the 3D CFD analysis is imposed on the flapping wing as the external loads. The peak of the strain energy is minimized in dynamic topology optimization. The number of the time steps near a peak is set by five and ESLSO is used for dynamic topology optimization. The results of the dynamic topology optimization are illustrated in Fig. 15.

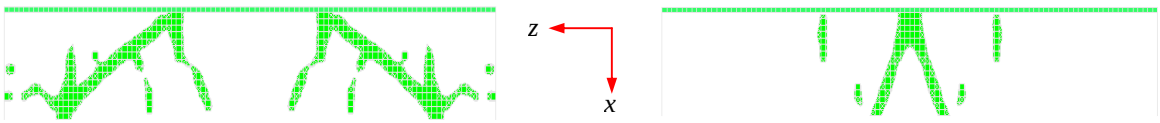

a) **b)**

Fig. 15 The results of dynamic topology optimization: a) Mass fraction: 0.1, b) Mass fraction: 0.05

Figure 15 a) is the result of dynamic topology optimization of the flapping wing when the mass fraction is 0.1, ε_1 is 0.3, ε_2 is 0.2 and ε_3 is 0.00001. Figure 15 b) is the results of dynamic topology optimization when the mass fraction is 0.05, ε_1 is 0.1, ε_2 is 0.1 ε_3 is 0.00001. The remaining elements show the distribution of the reinforcement of the wing.

The structure of the flapping wing should have some flexibility as well as certain rigidity and a small amount of rigidity guarantees flexibility [38-40]. However, how flexible or rigid the wing should be is not fully studied yet for each flapping wing. This research only shows that the results of dynamic topology optimization enable to keep a certain rigidity with a specific mass. If we know the target rigidity, topology optimization can be performed to meet the target rigidity. This aspect will be explained in the next section.

V. Future Direction for the Design of the Flapping Wing

This study shows the possibility of optimizing the flapping wing system. However, all the involved disciplines are separately considered. Therefore, the optimum solution is obtained in a local sense. In the future, they should be considered simultaneously. A direction of the future study is illustrated in Fig. 16. To include the stiffness of the structure, path optimization should be simultaneously performed with structural optimization, and aeroelasticity analysis is required in this process. A high fidelity structural model may cost too much in this optimization process. A low fidelity (simplified) structural model can be exploited. The approximation method of this research can be

utilized. Then the target for rigidity is evaluated and dynamic topology optimization is performed to meet the target. The external loads are made by the method of this research. For a final detailed design, size/shape optimization is performed to meet the target while various design conditions are satisfied. Eventually, multi-disciplinary design optimization (MDO) will be employed because the disciplines are coupled.

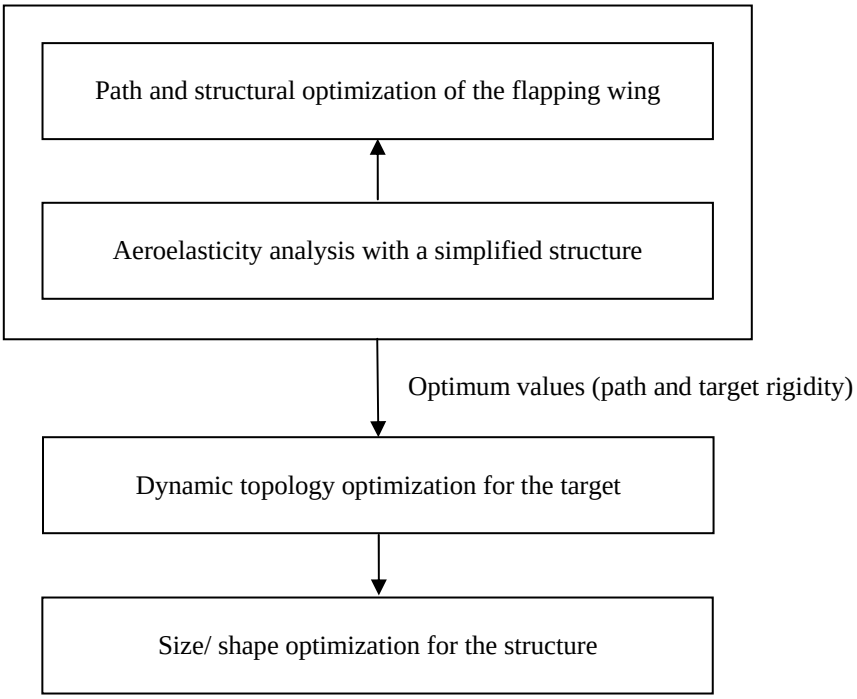

Fig. 16 Scenario for future direction.

VI. Conclusions

A flapping system is optimized and path optimization is conducted to enhance the performances such as thrust and propulsive efficiency. The Kriging method is employed for optimization and CFD analysis for a 2D airfoil is utilized for the optimization process. The determined path is utilized for dynamic topology optimization of the wing structure. The peaks of the strain energy are minimized to find the stiffest structure. The external loads are calculated from a 3D CFD airfoil analysis. Reinforcement within the wing is determined to have certain rigidity with minimum mass. Since the external loads are dynamically imposed in the time domain, a dynamic topology

optimization method is developed by using the equivalent static loads. Since the research is in the early stage, future direction for the research is proposed.

Acknowledgements

This research was supported by AOARD (AOARD-09-4103). The PI is thankful to Mrs. MiSun Park for her English correction of the manuscript.

References

[1] McMichael, J. M., and Francis, M. S., "Micro Air Vehicles – Toward a New Dimension in Flight," *DARPA*, USA, 1997.

[2] Garrick, I. E., "Propulsion of a Flapping and Oscillating Airfoil," *NACA Report*, No. 567, 1937.

[3] Young, J., Walker, S. M., Bomphrey, R. J., Taylor, G. K., and Thomas, L. R., "Details of Insect Wing Design and Deformation Enhance Aerodynamic Function and Flight Efficiency," *Science*, Vol.325, No.5947, 2009, pp. 1549-1552.

[4] Jones, K. D., and Platzer, M. F., "Bio-Inspired Design of Flapping Wing Micro Air Vehicles – An Engineer's Perspective," AIAA Paper, AIAA-2006-0037.

[5] Anderson, J. M., Streitlien, K., Barrett, D. S. and Triantafyllou, M. S., "Oscillating Foils of High Propulsive Efficiency," *Journal of Fluid Mechanics*, Vol. 360, 1998, pp. 41-72.

[6] Pesavento, U., and Wang Z. J., "Flapping Wing Flight Can Save Aerodynamic Power Compared to Steady Flight," *Physical Review Letters*, 118102, 2009, pp. 1-4.

[7] Tuncer, H. I., and Kaya, M., "Optimization of Flapping Airfoils for Maximum Thrust and Propulsive Efficiency," *AIAA Journal*, Vol. 43, No. 11, 2005, pp. 2329-2336.

[8] Kaya, M., and Tuncer, H. I., "Nonsinusoidal Path Optimization of a Flapping Airfoil," *AIAA Journal*, Vol. 45, No. 8, 2007, pp. 2075-2082.

[9] Kaya, M., Tuncer, H. I., Jones, D. K., and Platzer, M., "Optimization of Flapping Motion Parameters for Two Airfoils in a Biplane," *Journal of Aircraft*, Vol. 46, No. 2, 2009, pp 583-592.

[10] Soueid, H., Guglielmini, L., Airiau C., and Bottaro A., "Optimization of the Motion of a Flapping Airfoil Using Sensitivity Functions," *Computers & Fluids*, Vol. 38, 2009, pp. 861-874.

[11] Simpson, T. W., Mauery, T. M., Korte, J. J., and Mistree, F., "Kriging Models for Global Approximation in Simulation-Based Multidisciplinary Design Optimization," *AIAA Journal*, Vol. 39, No. 12, 2001, pp. 2233-2241.

[12] Queipo, N. V., Haftka R. T., Shyy, W., Goel T., Vaidyanathan R., and Tucker. P. K., "Surrogate-Based Analysis and Optimization," *Progress in Aerospace Sciences*, Vol. 41, 2005, pp. 1-28.

[13] Stanford, B., Ifju, P., "Aeroelastic Topology Optimization of Membrane Structures for Micro Air Vehicles," *Structural and*

Multidisciplinary Optimization, Vol. 38, No. 3, 2009, pp. 301-316.

[14] Choi, W. S., and Park, G. J., "Transformation of Dynamic Loads into Equivalent Static Loads Based on Modal Analysis," *International Journal of Numerical Method in Engineering*, Vol. 46, No. 1, 1999, pp. 29-43.

[15] Kim, Y. I., Park, G. J., Kolonay, R. M., Blair, M., and Canfield, R. A., "Nonlinear Dynamic Response Structural Optimization of a Joined-Wing Using Equivalent Static Loads," *Journal of Aircraft*, Vol. 46, No. 3, 2009, pp. 821-831.

[16] Park, G. J., "Technical Overview of the Equivalent Static Loads Method for Non Linear Static Response Structural Optimization," accepted by Structural and Multidisciplinary Optimization.

[17] ANSYS FLUENT, *User's Guide*, Ver. 12.1, ANSYS Inc, 2009.

[18] MD R3 Nastran, *User's Guide*, MSC. Software Corporation, 2008.

[19] GENESIS, *Software Package*, Ver. 10.0, Vanderplaats Research and Development, Inc., Colorado Springs, CO, 2008.

[20] The MATLAB help files, the Mathworks Company, 2009.

[21] Stroustrup, B, *The C++ Programming Language*, Addison Wesley, U.S.A, 2000.

[22] Miao, J. M., Ho, M. H., "Effect of Flexure on Aerodynamic Propulsive Efficiency of Flapping Flexible Airfoil," *Journal of Fluids and Structures*, Vol. 22, 2006, pp. 401-419.

[23] Heathcote, S., Wang, Z., and Gursul, I., "Effect of Spanwise Flexibility on Flapping Wing Propulsion," *Journal of Fluids and Structures*, Vol. 24, Issue 2, 2008, pp. 183-199.

[24] Bensoe, M. P., and Sigmund, O., *Topology Optimization: Theory, Methods and Application*, Springer, Germany, 2002.

[25] Jang, H. H., Lee, H. A., and Park, G. J. "Preliminary Study on Linear Dynamic Response Topology Optimization Using Equivalent Static Loads," *Transactions of the KSME*, Vol. 33, No. 12, 2009, pp. 1357-1493. (in Korean)

[26] GAMBIT, *User's Guide*, Ver. 2.3.16, Fluent Inc, 2006.

[27] Kinsey, T., Dumas, G., "Parametric Study of an Oscillating Airfoil in a Power-Extraction Regime," *AIAA Journal*, Vol. 46, No. 6, 2008, pp.1318-1330.

[28] Tuncer, I. H., and Kaya, M., "Thrust Generation Caused by Flapping Airfoils in a Biplane Configuration," *Journal of Aircraft*, Vol. 40, No. 3, 2003, pp. 509-515.

[29] Tang, J., Chimakurthi, S., Palacios, R., Cesnik C., Shyy W., "Computational Fluid-Structure Interaction of a Deformable Flapping Wing for Micro Air Vehicle Applications," AIAA-2008-0615.

[30] Wang, Z. J., Birch, J. M., and Dickinson, M. H., "Unsteady Forces and Flows in Low Reynolds Number Hovering Flight: Two-Dimensional Computations *vs* Robotic Wing Experiments," *The Journal of Experimental Biology*, Vol. 207, 2004, pp. 449-460.

[31] Park, G. J., *Analytic Methods for Design Practice*, Springer, Berlin, 2007.

[32] Min, S., Kikuchi, N., Park, Y. C., Kim, S., and Chang, S., "Optimal Topology Design of Structures Under Dynamic Loads," *Structural and Multidisciplinary Optimization*, Vol. 17, No. 2-3, 1999, pp. 208-218.

[33] Park, G. J., and Kang, B. S., "Validation of a Structural Optimization Algorithm Transforming Dynamic Loads into Equivalent Static Loads," *Journal of Optimization Theory and Applications*, Vol. 119, No. 1, 2003, pp. 191-200.

[34] Park, K. J., Lee, J. N., and Park, G. J., "Shape Optimization Under Static Loads Transformed from Dynamic Loads," The Fifth World Congress of Structural and Multidisciplinary Optimization, May 19 – 23, Lido di Jesolo, Italy, 2003, pp. 219-220.

[35] Shin, M. K., Park, K. J., and Park, G. J., "Optimization of Structures with Nonlinear Behavior using Equivalent Loads," *Computer Methods in Applied Mechanics and Engineering*, Vol. 196, Issues 4-6, 2007, pp. 1154-1167.

[36] Kang, B. S., Park, G. J., and Arora, J. S., "Optimization of Flexible Multibody Dynamic System Using the Equivalent Static Load Method," *AIAA Journal*, Vol. 43, Issue 4, 2005, pp. 846-852.

[37] Kim, Y. I., and Park, G. J., "Nonlinear Dynamic Response Structural Optimization Using Equivalent Static Loads," *Computer Methods in Applied Mechanics and Engineering*, Vol. 199, Issues 9-12, 2010, pp. 660-676.

[38] Combes, S. A., Daniel, T. L., "Flexural Stiffness in Insect Wings I: Scaling and the Influence of Wing Venation," *The Journal of Experimental Biology*, Vol. 206, No. 17, 2003, pp. 2979-2987.

[39] Kim, D. K., Han, J. H., "Optimal Design of a Flexible Flapping Wing Using Fluid-Structure Interaction Analysis," The 8th International Conference on Motion and Vibration Control, TUM, Munich, Germany, Sep. 15-18, 2008.

[40] Heathcote, S., Wang, Z., and Gursul, I., "Effect of Spanwise Flexibility on Flapping Wing Propulsion," *Journal of Fluids and Structures*, Vol. 24, Issue 2, 2008, pp. 183-199.